

EXPERIMENTAL INVESTIGATION AND SIMMER-III CODE MODELLING OF LBE-WATER INTERACTION IN LIFUS5/MOD2 FACILITY

ABSTRACT

In the frame of the THINS Project, an experimental campaign was performed on LIFUS5/Mod2 facility at ENEA RC Brasimone, aiming to investigate the water-LBE interaction. Such a phenomenon occurs as consequence of a postulated Steam Generator Tube Rupture event in a HLMFR system. Four tests were performed injecting sub-cooled water at 40 bar into a reaction vessel partially filled by low pressure LBE at 400°C.

The post-test activity was performed by the SIMMER III code in order to improve the understanding of the involved phenomena and to confirm the code capabilities in simulating the water-LBE interaction. The calculated data showed a qualitatively agreement with the measured values and a faster reaction kinetics due to the modelling assumptions.

KEYWORDS

Steam Generator Tube Rupture, Coolant Coolant Interaction, water LBE interaction,

NOMENCLATURE

ADS	Accelerator Driven Systems
CCI	Coolant Coolant Interaction
E-BIC	Experimental Boundary and Initial Conditions
HLMFR	Heavy Liquid Metal Fast Reactor
LBE	Lead Bismuth Eutectic
L-M	Lockhart-Martinelli
PHX	Primary Heat Exchangers
SG	Steam Generator
SGTR	Steam Generator Tube Rupture
TC	Thermocouple
THINS	Thermal Hydraulic of Innovative Nuclear System

1 INTRODUCTION

The new generation Heavy Liquid Metal Fast Reactors (HLMFRs) and Accelerator Driven Systems (ADSs) are currently designed as pool type reactor, implementing the Steam Generators (SGs) or Primary Heat Exchangers (PHXs) into the primary pool, where also the core, primary pumps and main components are set (*C. Fazio et al., 2006*), (*L. Cinotti et al., 2007*). This design feature allows increasing the reactor performance and simplifying the whole layout, by complete removal of intermediate circuit. In such a configuration the secondary coolant (water), entering in the heat exchanger tube bundle at high pressure and sub-cooled conditions, could come into contact with the primary heavy liquid metal coolant, at higher temperature and lower pressure, in a postulated Steam Generator Tube Rupture (SGTR) accident.

The SGTR event entails pressure waves propagation and cover gas pressurization, that could compromise the structural integrity of the surrounding components. Moreover, the rupture of a single SG tube could affect, in principle, the integrity of the neighbouring tubes (domino effect), making worse the consequences of the accidental scenario. The SG-shell constitutes a shield to the pressure wave propagation into the LBE melt. Its dumping effect

needs to be studied and calibrated in concert with the implemented safeguard devices, as rupture disks and fast valves set on the vessel dome, flow limiters on the feed-water (Venturi nozzle) and SGTR detectors. The SGTR event, thus, should be considered as a safety issue in the design and preliminary safety analysis. This requires availability of qualified experimental data, having two main purpose: a) direct extrapolation to full scale nuclear plant conditions, if the facility geometry, configuration and the experimental initial and boundary conditions are properly scaled and representative of the reactor prototype; b) supporting the development and demonstrating the reliability of specific computer codes in simulating multi-fluid multi-phase problems by means of high-quality measurement data.

In the frame of THINS Project, ENEA RC Brasimone performed experimental campaign aiming to provide high quality data in LIFUS5/Mod2 facility for investigating the HLM/water interaction, developing and validating physical modelling and for improving and qualifying computer codes in relevant conditions for SGTR event. LIFUS5/Mod2 is a separate effect test facility re-constructed on the basis of the operating experience on LIFUS5.

This paper describes the LIFUS5/Mod2 facility, the implemented instrumentation, the final THINS test matrix and the high pressure tests carried out in the framework of the EC funded THINS Project (A. Del Nevo et al., 2013a), (A. Del Nevo et al., 2013b), (A. Del Nevo et al., 2013c) and (A. Del Nevo et al., 2013d).

The post-test analysis was performed by the axial-symmetric SIMMER III code. It is up to eight velocity fields, multi-component, multiphase, Eulerian fluid-dynamics code coupled with a space and energy dependent neutron kinetics model (Y. Tobita et al., 2002), (S. Kondo et al., 2003). The code was originally developed to deal with Core Disruptive Analysis in Liquid Metal Fast Reactor and over the years its range of applications was extended including issues related to advanced fast reactors, steam explosion and fuel coolant interaction phenomena. The capability of the SIMMER III code to reproduce the phenomenology of the LBE-water interaction was studied and highlighted by previous activities performed at ENEA-Brasimone in collaboration with University of Pisa (A. Ciampichetti et al., 2008), (A. Ciampichetti et al., 2009), (A. Ciampichetti et al., 2011).

2 LYFUS5/MOD2 FACILITY

LIFUS5/Mod2 facility, see Figure 1, was designed to operate with heavy liquid metals, such as: Lithium-Lead alloy, Lead-Bismuth eutectic alloy and pure lead. The operation of the test facility has the objectives of 1) investigating relevant phenomena connected with the safety of HLM fast reactor designs and 2) developing and validating numerical models for simulation codes used in safety analysis.

LIFUS5/Mod2 consists of two main parts: a reaction vessel (S1), where LBE / water interactions occurs and a water tank (S2) pressurized by means of a gas cylinder connected on the top. The main features of the components characterizing LIFUS5/Mod2 facility are summarized in Table 1.

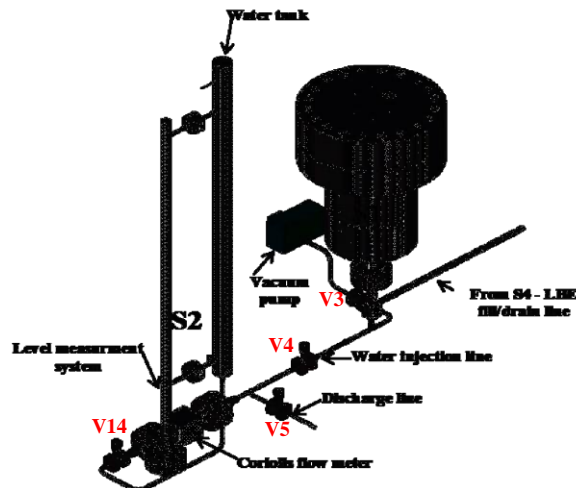


Figure 1: LIFUS5/Mod2 overall sketch

Table 1: LIFUS5/Mod2 main features of components

SYSTEM S1		INTERACTION VESSEL
S1-1	Volume [m ³]	0.1
S1-2	Inner diameter [m]	0.42
S1-3	Height [m]	1.085
S1-4	Design pressure [bar]	200
S1-5	Design temperature [°C]	500
S1-6	Material	AISI 316
SYSTEM S2		WATER TANK
S2-1	Volume [m ³]	0.015
S2-2	Diameter	4 inch sch. 160
S2-3	Design pressure [bar]	200
S2-4	Design temperature [°C]	350
S2-5	Material	AISI 316

The main vessel S1 (see Figure 1) is about 100 litres, and it is partially filled with LBE. It is closed by the top flange sealed by a Garlock HELICOFLEX. Internally, S1 can be divided into an upper cylindrical part and a lower hemispherical part. The main diameter is 420 mm and the overall height is 780 mm. A coaxial penetration at S1 bottom allows the water injection and LBE charge/discharge, see Figure 2.

A support frame composed of four horizontal cruciform levels is welded coaxially to S1 flange (see Figures 2 and 3), on which 68 thermocouples are positioned. The overall height of the frame is 590 mm. The thermocouples positioning is highlighted by red dots in Figure 3. The lower cruciform support, Level 1, is the nearest to the injection orifice and it has a vacuum (the central thermocouple is absent) in the central position to avoid the impact with the water jet. The second level, like the higher ones, reaches the axis of the structure and a thermocouple is positioned at the centre. Therefore, it constitutes an obstacle that fragments the water jet flowing upwards into the LBE melt.

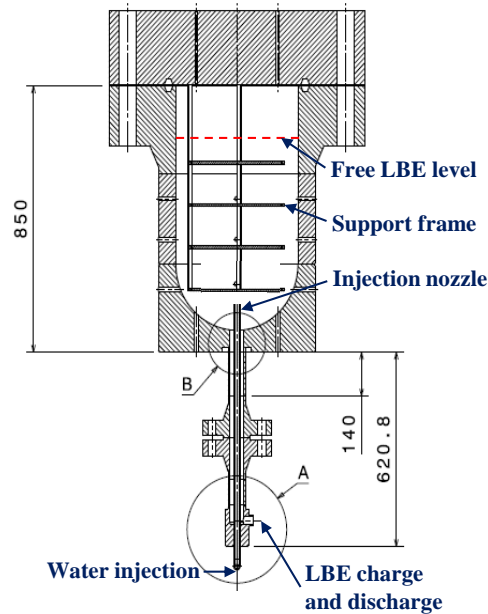


Figure 2: LIFUS5/Mod2 facility, injection system

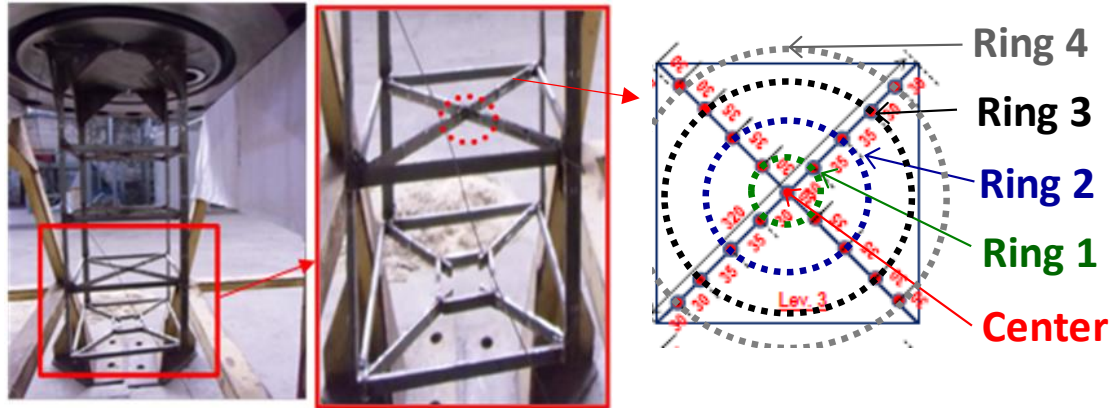


Figure 3: Support structure of the thermocouples in S1

Each one of the four horizontal branches constituting the cruciform support, hosts four thermocouples. The thermocouples nearest to the central one are considered belonging to the first ring, the outer ones to the fourth ring, see Figure 3.

The injection is carried out about 120 mm above the internal lower edge of S1 vessel. The injector orifice is covered by a protective cap, which is broken by the increasing pressure at the beginning of the injection phase. Therefore, the system shall be substituted at the end of each test. The injection orifice has a diameter equal to 4 mm and it is mounted at the end of the water injection line based on a 1/2" sch 80 pipeline.

The water line connects the tank S2 with the interaction vessel S1 and the vacuum pump line. In the middle a discharge valve (V5) is installed, for draining the water at the end of the tests, and for removing steam formation during the conditioning heating phase.

As shown in Figure 1, the water flows from S2 towards the valve V14, then the Coriolis flowmeter and finally through valve V4, before it enters in S1. Valve V3 is placed between the pump and the water line. Before the injection occurs, the vacuum pump is activated to remove the gas in the injection line. In this way, the conduct between V14 and V3 results filled by low pressure air when the water injection starts (V14 opening). Therefore, the injected high pressure water expands and evaporates flowing toward the vessel S1.

Along the path of the water two-phase flow occurs, the evaporation magnitude affects significantly the pressure drops in the injection line, that affect the amount of water injected in S1 and consequently its pressurization kinetics. The water tank S2 is a 4 inch sch. 160 pipe, having a volume of 14 litres, it is closed at the edges with proper welded plugs. It is connected on the top with the gas line, which is used for setting and keeping the pressure of the water according with the test specifications. The vessel S2 is connected by means of two lateral flanges on a magnetic level measurement device.

2.1 Instrumentation, control and data acquisition systems

The instrumentation, control and data acquisition systems of LIFUS5/Mod2 facility were upgraded for improving the level of details of the parameters involved in the phenomena of interest, as well as for providing to code developers/users more reliable definition of the initial and boundary conditions.

Three types of measurements were planned in the facility and utilized for the acquisition, control and regulation system.

The instrumentation for the interaction vessel (S1) is composed by: 68 low time constant thermocouples (TC), for fast temperature acquisition, installed on the support structure inside the vessel S1, providing measures at different radial, azimuthal and axial positions; 5 fast pressure transducers, one on the top of the vessel and four on the vessel

wall at different elevations; 6 high temperature strain gauges installed on the reaction vessel, five of which on the internal wall at different heights and one externally.

The instrumentation for the water injection system is composed by: 1 level measurement gauge, mounted on the water tank support, having maximum resolution of 20-25 g in the THINS experimental campaign conditions; 2 fast pressure transducers, placed on the bottom of the water tank and on the water injection line downstream the last valve V4; 3 thermocouples, one of which in the dome of the water tank, the second one in the water side of S2 and the third one downstream the injection valve, near valve V3; 1 Coriolis flowmeter placed on the water line between the valves V14 and V4, to provide an accurate measurement of the mass flow of the water injected.

Besides the instrumentation of the acquisition system, the control and regulation systems provide also some data to the acquisition system by means of: 1 absolute pressure transducer on the top flange of S1; 2 thermocouples on the vessel wall of S1; 3 absolute pressure transducers installed in the gas zone of S2 tank and in the gas line close to the gas cylinder.

3 THINS TEST MATRIX

The overall THINS experimental campaign is composed of two series of tests, characterized by water tank (S2) pressure set at 40 and 16 bar, respectively. Only the analysis of the high pressure tests is presented in this study. The test matrix definition foreseen three quantities for performing single variant tests: temperature of the injected water, gas argon to LBE volume ratio in S1 and total amount of injected water, i.e. the opening time of the injection valve. Table 2 summarizes the specifications of THINS test matrix.

Table 2: High pressure THINS test matrix

#	E-BIC	T#1	T#2	T#3	T#4
1	Interaction system	S1	S1	S1	S1
2	LBE temperature [°C]	400	400	400	400
3	Water pressure [bar]	40	40	40	40
4	Water temperature [°C]	240	200	240	240
5	Argon volume/LBE volume [%]	30	30	40	30
6	Lasting time of the injection valve on [s]	~2.5	~2.5	~2.5	~2.5
7	Water injection penetration in S1 [mm]	120	120	120	120
8	Injector orifice diameter [mm]	4	4	4	4

The main outcomes of the experimental campaign were the generation of detailed and reliable experimental data, improvement of the knowledge of physical behaviour and involved phenomena, investigation of dynamic effects of energy release on the structures and enlargement of database for code validation.

The test section details, the exact experimental boundary conditions and the pressure and temperature time trends measured during the transients were published by specific ENEA reports (A. Del Nevo et al., 2013a), (A. Del Nevo et al., 2013b), (A. Del Nevo et al., 2013c), (A. Del Nevo et al., 2013d).

4 SIMMER III MODEL

The SIMMER III code can deal with safety analysis problems in advanced fast reactors and constitutes one of the few codes able to simulate the coolant-coolant interaction (CCI), taking into account the water evaporation occurring during the penetration into liquid metals.

The SIMMER III geometrical domain is shown on the left side of Figure 4, the main components of which are connected by dashed arrows to the real components shown in the LIFUS5/Mod2 overall sketch on the right of the same figure, for sake of clarity. The geometrical domain is obtained by 23 radial and 88 axial subdivisions. The LBE is represented in red, the water in blue, the argon (cover gas) and air (injection line) in white and the non-calculation regions in light green. Rotating the 2D SIMMER domain along the axis of symmetry (blue dot-dashed line) the whole volumetric model is obtained, in which every cell is a toroidal volume with rectangular section.

The reaction vessel S1 was positioned in the upper part and coaxially to the model. The injection line is horizontally installed and cannot be coherently modelled in an axisymmetric domain, therefore, to conserve the cylindrical shape of the injection tube, it was positioned vertically and coaxially with the entire model. The injection tube length is almost equal to 4 m, this value has been conserved in vertical direction and due to the water density, in THINS conditions, the simplification performed entails almost 0.4 bar of gravity pressure losses in the SIMMER model that do not occur in the experimental conditions. This simplification has been considered acceptable due to the considerably higher water pressure, i.e. 40 bar. The vertical injection line (1/2 inch of diameter) penetrates 120 mm into the vessel S1, at the top of this line the orifice with diameter of 4 mm is set. On the left of Figure 4, the positions of the valve V14, V4 and the 2 inch tube, where the Coriolis flow meter is set, are shown.

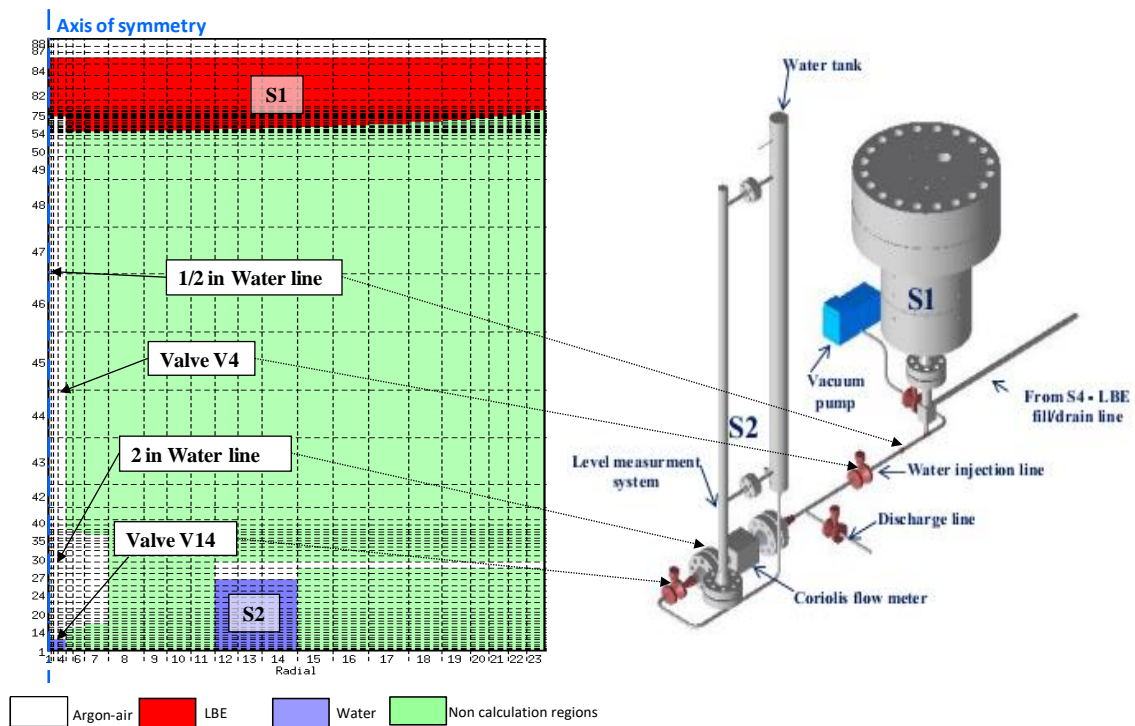


Figure 4: SIMMER III geometrical model

The pressure time trends measured in the S2 dome were imposed as computational boundary condition of the simulations.

The SIMMER model shown in Figure 4 depicts the calculation start instant ($t = 0$ s), when the water begins to flow through the injection valve V14 and evaporates in the downstream low pressure conduct. At the top of which, the injection orifice is kept closed for the lapse of time experimentally measured to achieve the cap rupture. The interruption of the water injection was simulated, as it occurred during the tests, by the valve V4 closure, which isolates the vessel S1 from the pressurized water tank S2.

The injection line was implemented in the SIMMER model delimited by non-calculation regions. It implies that the fluid-structure coupling does not occur and consequently the pressure drops along the injection line are not directly computed by the code. In such a simplified configuration the single phase pressure drops were modelled by concentrated pressure drops simulated by means of orifice coefficients. This approximation does not allow the two phase pressure drops prediction in the injection line.

5 SIMMER III CODE RESULTS

The results obtained by the SIMMER III code for tests T#1, T#2, T#3 and T#4 are shown hereafter. The depicted experimental and calculated pressure time trends are differentiated by colours. The measured data in the dome of the water tank, reaction vessel S1 and injection line are azure, green and grey, respectively, the calculated values in the supply line and S1 are depicted in red and blue, respectively.

The experimental and calculated pressure time trends of the **test T#1** (named A1.2_1 in the ENEA report (*A. Del Nevo et al., 2013b*)) are shown in Figure 5.

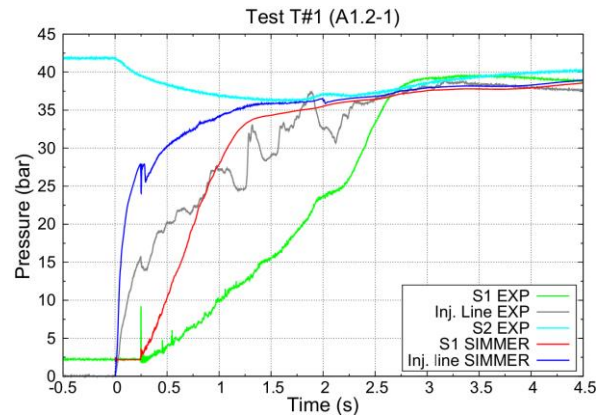


Figure 5: Calculated and experimental pressure time trends of the test T#1

The computed values over-predict the measured data. The opening of the injection orifice occurs almost 0.25 s after the water injection start, at this instant the computed pressure in the injection line overestimates the calculated one of almost 12 bar. It is due to the lower pressure drops simulated along the injection line of the SIMMER model. It also entails a calculated pressure time trend in S1 with a higher slope than the measured one. The kinetics of the pressure transient results therefore accelerated and the SIMMER code predicts the pressure plateau almost 1 s earlier. The tests T#1 and T#4 were performed imposing almost the same boundary and initial conditions. However, comparing Figure 5 and Figure 12, the experimental pressure time trends measured into the reaction tank differ by almost 10 bar at about 1.5 s after the injection starting. This inconsistency could be attributed to the different instant at which the cap rupture occurs and the consequent different injection line pressurization reached, as well as the uncertainty about the cap rupture dynamics. The calculated data of these tests (red lines), instead, show pressurization time trends in agreement between them.

The SIMMER code predicts an overall water mass injected into S1 almost equal to 0.36 kg. This value is reasonably in agreement with that experimentally estimated of 0.42 kg (*A. Del Nevo et al., 2013b*). The higher computed pressurization of S1, indeed, reduces the amount of water injected into the reaction tank, showing the consistency of the numerical result with the experimental one.

The investigation of the vapour bubble formation and growth in the reaction tank was performed and is shown in Figure 6. The LBE volume fraction ranging from 1 to 0 is depicted in red and in blue respectively. The instant in which the vapour bubble, created by the vaporization of the water injected in S1, enters the cover gas region entails the loss of meaning of the cover gas compression work computed by the SIMMER post processor BFCAL. It justifies the zoom to the first tenths of second in Figures 8 and 9. As shown in Figure 6, the vapour bubble reaches the cover gas almost 0.4 s after the start of the simulation, that is almost 0.15 s after the water entrance into S1.

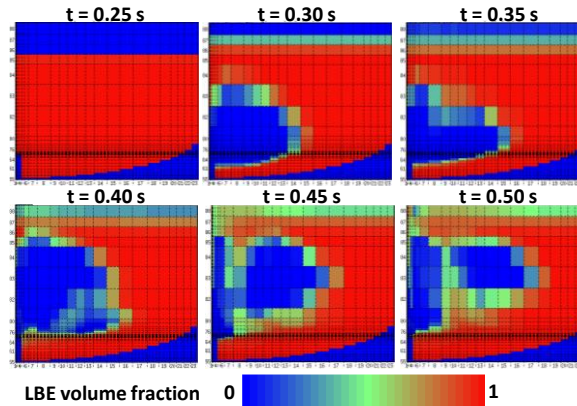


Figure 6: Water and vapour bubble in S1, by SIMMER III code

The instant in which the rupture of the vapour bubble occurs could be more precisely identified, as shown in Figure 7, by the observation of the water kinetic energy time trend in the cover gas region (red line) becoming higher than zero. In the same figure, also the water kinetic energy trend in the LBE region is depicted (blue line). The computed water kinetic energies have low values, having the order of magnitude of the Joule in the LBE and tenths of Joule in the cover gas region (Figure 7).

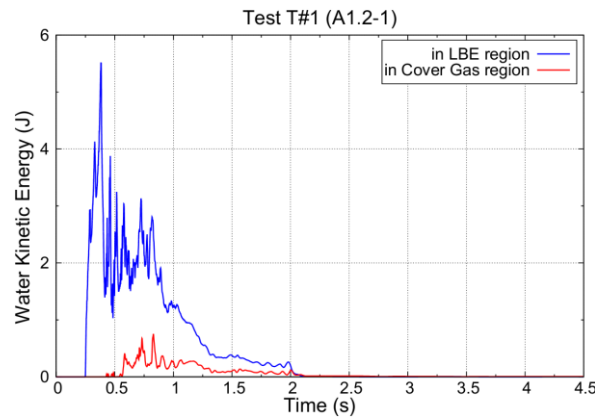


Figure 7: Water kinetic energy time trends in the cover gas and LBE regions, calculated by SIMMER III code

Due to the lack of meaning of the cover gas energy content after the entering of an external gas (vapour), the mechanical energy (blue line), compression work (red line) and total kinetic energy (green line) are depicted in Figure 8 up to 0.6 s after the calculation start. The sum of the total kinetic energy and the compression work in the cover gas region provides the mechanical energy (blue line). The compression work time trend shows an oscillating behaviour due to action of the cover gas that tends to counteract the upward movement of LBE. Figure 8 shows also that kinetic energy constitutes a lower part of the mechanical energy, which is mainly constituted by the compression work of the cover gas.

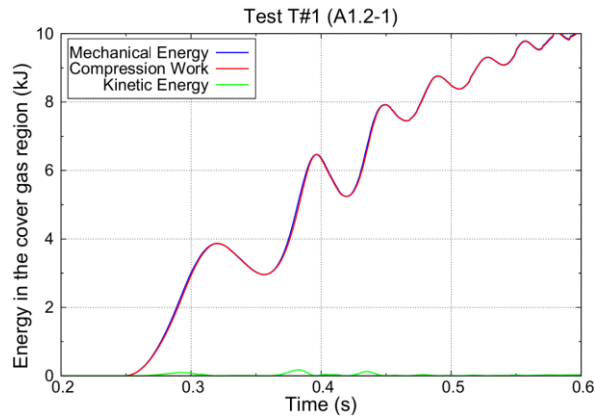


Figure 8: Mechanical energy, compression work and kinetic energy time trends in the cover gas region, calculated by SIMMER III code

Comparing the components of the mechanical energy in the reaction vessel S1, see Figure 9, it is possible to note that the compression work presents a relative maximum or minimum in coincidence of the relative minimum of kinetic energy and the maximum compression work time derivative (compression power) is coincident with the relative maximum kinetic energy.

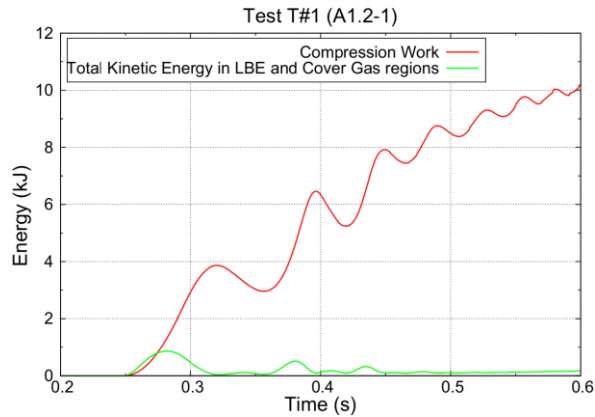


Figure 9: Compression work and kinetic energy time trends in the reaction vessel S1, calculated by SIMMER III code

The experimental and calculated pressure time trends of **test T#2** (named A1.3 in the ENEA report (A. Del Nevo et al., 2013c)) are depicted in Figure 10. Analysing the SIMMER results, it can be seen that the code overestimates the pressures measured in S1 and injection line.

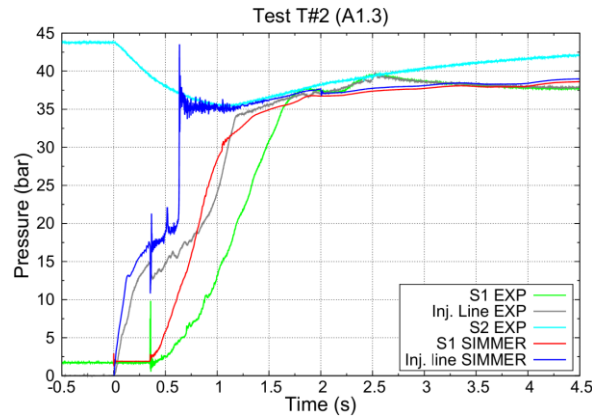


Figure 10: Calculated and experimental pressure time trends of the test T#2

In particular, it is possible to note that the computed pressure in the injection conduct, blue line, before the orifice opening, overestimates slightly the experimental data. This difference is lower than in the tests T#1, T#3 and T#4 because of the lower water evaporation occurring in the test T#2 into the injection line, due to the lower water temperature: 200°C instead of 240°C.

After the orifice opening, the blue line has a slope in agreement with the experimental grey one up to almost the instant $t = 0.6$ s, when the liquid water single-phase flow is established in the modelled injection line and the pressure in the injection line increases, becoming slightly lower than that of the water tank. The calculated rapid transition from two- to single-phase flow anticipates of almost 0.4 s the gradual experimental phenomenon. Such an abrupt change of flow regimes entails a numerical pressure peak of almost 43 bar.

The total water mass injected into the reaction vessel S1 has been computed by SIMMER code to be almost 0.4 kg, that is coherent with the value experimentally estimated.

Analogously to the previous test, the vapour formation and growth in S1 and energy analysis were performed. The water injected at low temperature (200°C) entails lower water evaporation in S1 and consequently a higher water kinetic energy in comparison with the tests T#1, T#3 and T#4. The oscillation of the energy related time trends, i.e. energy components in the cover gas and S1, has lower frequency and magnitude compared with the previous test. Since the injection of higher sub-cooled water slows down the kinetics of the LBE-cover gas interaction.

Test T#3 (A1.1 in the ENEA report (*A. Del Nevo et al., 2013a*)) was performed increasing the cover gas fraction (40% of the LBE volume). The measured and calculated pressure time trends are shown in Figure 11.

The higher free volume in S1, with respect to the other tests, entails a measured lower pressure value at the end of transient, almost 32 bar, and slows down the kinetics of the transient.

The calculated pressure time trends overestimate the experimental data during the first 3 s after the valve V14 opening, they are however qualitatively in agreement. The calculated pressure values are, instead, in good agreement with the experimental ones after the pressurization of the reaction vessel was reached, at almost $t = 3$ s.

At the instant of the orifice opening, the pressure computed in the injection line overestimates the measured one by almost 10 bar. The analogous difference in the test T#2 was almost a third, due to the higher water sub-cooling that entails a lower evaporation along the injection line.

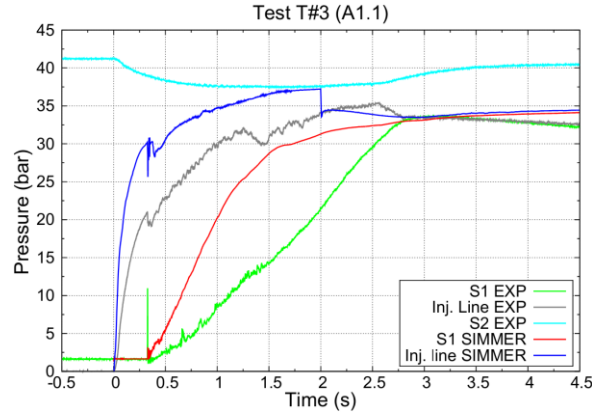


Figure 11: Calculated and experimental pressure time trends of the test T#3

The overall computed water mass injected is about 0.5 kg, coherently with the measured value. It is also consistent with the other tests, because the lower S1 pressurization allows that a higher quantity of water was injected in the reaction vessel.

The vapour enters the cover gas at almost 0.7 s after the calculation start instant. This lapse of time is higher than in the other tests, because the higher cover gas volume defines a system having higher compressibility, in which the water kinetic energy in the cover gas, has values significantly higher than zero up to the end of the water injection (almost $t = 2$ s) and the water kinetic energy in the LBE region has initial lower values.

Test T#4 (A1.4 in the ENEA report (*A. Del Nevo et al., 2013a*)) has the same boundary and initial conditions of the test T#1. The calculated and experimental pressure time trends are shown in Figure 12. The pressure transducer set in the injection line did not work properly and measured data near to 0 bar, grey line close to the axis of abscissas. However, it is reasonable to assume, that before the orifice opening, the pressure trends in the injection line has a trend comparable to those measured during the test T#1 and T#3, with possible differences due to the instant in which the rupture of the cap occurs.

The numerical results obtained by the SIMMER code over-predict the experimental data during the phase of pressure increase in S1, similarly to the other tests. The plateaux computed at the end of the transient is in agreement with the measured data.

The calculated overall water mass injected during the transient is almost 0.37 kg. This value underestimates the measured data of 0.47 kg, because of the numerical faster pressurization of S1.

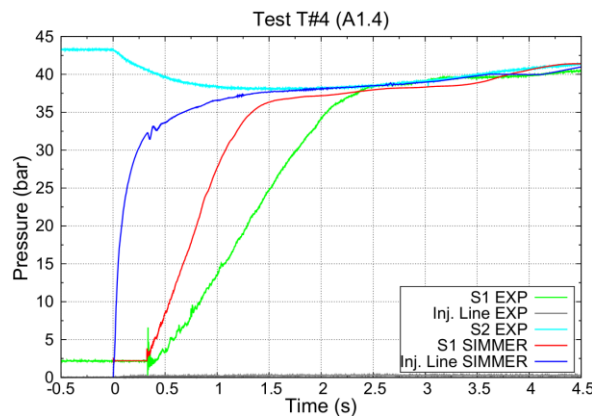


Figure 12: Calculated and experimental pressure time trends of the test T#4

The first tenths of second of the water injection into S1 provides numerical results in terms of energetic analysis analogous to those obtained for the test T#1.

The modelling of the injection line is at the basis of the pressure time trends overestimation, due to the underestimation of the two-phase pressure drops. Aiming to improve the obtained results, a rough application of the Lockhart-Martinelli multiplier has been done and the obtained results are shown in Figure 13.

The calculated pressure time trend into the reaction vessel S1 shows a considerable slope reduction in comparison with Figure 12 and the obtained results appear improved.

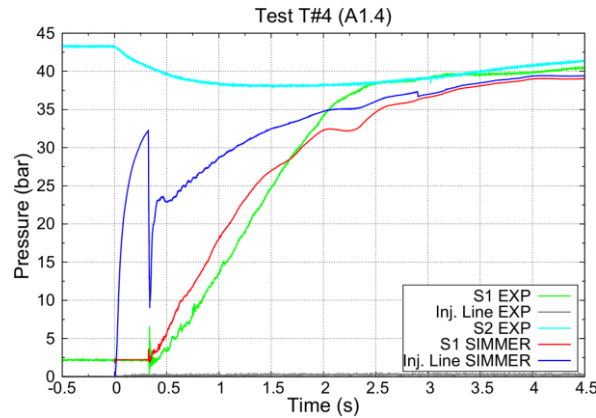


Figure 13: Calculated and experimental pressure time trends of the test T#4, with two-phase multiplier

The adopted method was applied multiplying the orifice coefficients, calculated and set in the model to take into account the single-phase friction pressure drops, by the Lockhart-Martinelli two-phase friction multiplier, evaluated at an average quality value, e.g. 0.3. It corresponds (assuming a unitary slip ratio) to a high void fraction, which becomes too high when the quality in the channel decreases. Indeed, the computed pressure trend in S1, red line in Figure 13, shows a slope decrease almost after the instant $t = 1.5$ s, because at almost 1.25 s liquid single phase occurs in the conduct. Therefore the calculation was restarted from almost 1.25 s setting the L-M multiplier equal to 1. The obtained results are shown in Figure 14 and appear to be in agreement with the experimental data, during the pressurization phase of the reaction vessel, as well as at the end of the transient, when almost stationary pressure values are reached.

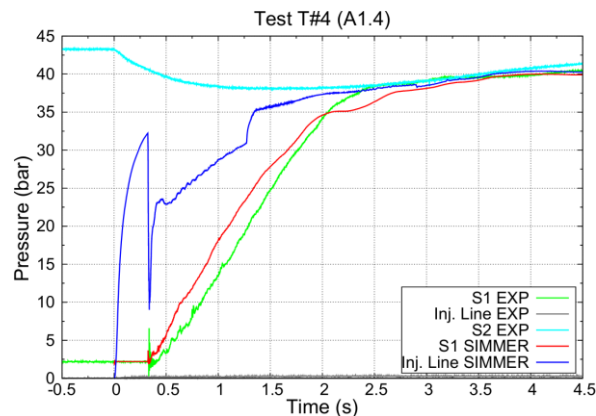


Figure 14: Calculated and experimental pressure time trends of the test T#4, with modified two-phase multiplier

The measured and computed **temperature time trends** of the corrected test T#4 (see Figure 14) are shown in Figures 15 and 16, by continuous and dotted lines, respectively. The temperatures measured in the centre, first,

second, third and fourth ring are depicted by red, green, blue, black and grey lines, respectively. In the legends, the radial and axial cell number in which the depicted trends are computed are provided between brackets.

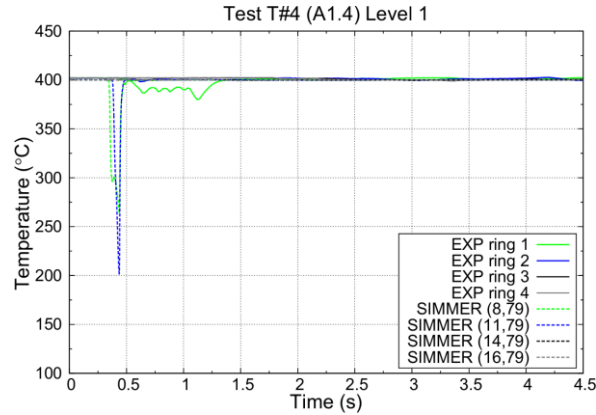


Figure 15: Experimental and calculated temperature time trends in the Level 1 of corrected test T#4

Figure 15 shows the measured and computed temperature on the first level of the support structure. The code provides an anticipated and higher cooling effect on the first and second TCs' ring. Due to the wider vapour jet predicted by the code at the injection start instants. The adopted default code settings appear thus unsuitable to take properly into account the expansion vapour kinetics in the LBE pool.

Figure 16 depicts the experimental and calculated temperature time trends on the second level. The central temperature, red line, has a trend comparable to the experimental data. Showing, however, an anticipated cooling effect and a delayed TC rewetting by hot LBE. The outer thermocouples are cooled until 0.5 s after the injection start. Instead, the measured data show a cooling effect on the first thermocouples ring (green line) until almost 3 s after the transient start.

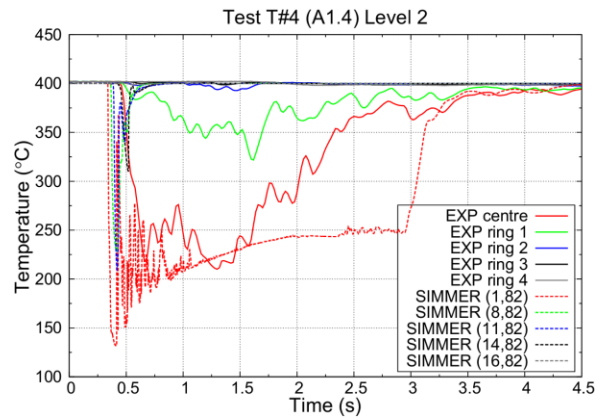


Figure 16: Experimental and calculated temperature time trends in the Level 2 of corrected test T#4

An underestimation of the central temperature was computed also at the third and fourth level, because, in the model, the water injected flows upwards undisturbed, due to the lack of the four horizontal cruciform supports. Because their geometry is not definable by an axisymmetric model. It would require the adoption of a three-dimensional model, feasible by the SIMMER IV code.

6 CONCLUSIONS

In the frame of the THINS project, an experimental campaign of four tests was carried out, aiming to study the water-LBE interaction on the LIFUS5/Mod2 facility at ENEA RC Brasimone.

The performed tests investigated the injection of 40 bar sub-cooled water into the reaction tank (S1) partially filled by LBE at low pressure and 400°C. The test section welded to the LIFUS5/Mod2 top flange was constituted by a frame supporting almost 70 thermocouples, aiming to evaluate the vapour flow path inside S1. The pressurization of the reaction tank was monitored by 5 fast pressure transducers. The experimental test matrix foreseen three quantities for performing single variant tests: temperature of the injected water, cover gas volume and opening time of the injection valve. The measured pressure time trends show a faster pressurization due to colder water injection and lower pressurization in case of higher cover gas volume, in comparison to the reference (first) test.

The post-test activity was carried out by the axisymmetric SIMMER III code. The modelling of LIFUS5/Mod2 was performed adopting simplifications concerning the injection line and thermocouples support. The key issue to obtain computational pressure time trends in agreement with the experimental data is constituted by a correct estimation of the two-phase pressure drops along the injection line. It was performed by a simplified application of the Lockhart-Martinelli multiplier and the obtained results show a pressure time trend in the reaction tank in agreement with the experimental data during the whole transient. The computed temperature time trends show a general cooling overestimation on the axis of S1. It is due to the impossibility to model by an axisymmetric code the four horizontal cruciform supports that constitute an obstacle against which the water jet impacts.

An improvement of the computed results could be obtained performing a three-dimensional model of the LIFUS5/Mod2 facility by the SIMMER IV code.

ACKNOWLEDGMENTS

The performed study was carried out in the frame of the THINS Project, funded by European Commission (FP7-EC) No. 249337. The support of EC is gratefully acknowledged. The authors wish to thanks all the ENEA's technicians involved in the implementation and operation of the LIFUS5 facility.